EXPERIMENTAL STUDY ON SEMI-RIGID PILE HEAD JOINTS OF CAST-IN-PLACE CONCRETE PILES

T. Yamamoto[1], N. Fukatsu[2], Y. Ban[2], K. Yamada[3] and T. Iida[4]

[1] *Professor, Dept. of Architecture, Daido Institute of Technology, Nagoya, Japan*
[2] *Researcher, Tech. Res. Inst. for Earthquake Eng., Yahagi Construction Co., Ltd., Nagoya, Japan*
[3] *Professor, Dept. of Architecture, Aich Institute of Technology, Toyota, Japan*
[4] *Manager, Japan Pile Corporation, Tokyo, Japan*
Email: [1] yamamoto@daido-it.ac.jp, [2] n-fukatsu@yahagi.co.jp

ABSTRACT :

To avoid the excessive input of earthquake loads through large piles it is useful to control the moment of piles by the head joints connecting to the bases. An experimental investigation was performed to examine the shear-flexural behaviors of moment controlled semi-rigid pile head joins of cast-in-place concrete piles. The proposed pile head joints that control the moment consist of the reduced concrete sectional area, short steel ring and reinforcing bars. The reduced concrete sectional area reduces the pile moment and the steel ring confines the concrete and controls the local destruction of the pile head joints. The cyclic lateral loads were applied to the specimens under a control of relative displacement angles (R) between the end stubs up to R=1/20. There was no damage in the head joints until R=1/100 and the shear-flexural behaviors were stable up to R=1/20. The experimental results showed that the proposed semi-rigid pile head joins were able to reduce the moment which occurs to the pile head and satisfy the seismic performance. A simple way to estimate the confined concrete strength and rotational performance of the semi-rigid pile heads are presented.

KEYWORDS: Pile head joint, Semi-rigid, Cast-in-place concrete pile

1. INTRODUCTION

As buildings become taller, piles become bigger in size. Hence, the large moment by big piles is input into the connected bases. Recently considerable structural damages of substructures caused by severe earthquakes have been reported (Yamakata, 1996). To avoid structural damage of substructures it is advisable to reduce the large pile moment. The semi-rigid pile head joints of cast-in-place concrete piles that are clear structurally and economical are proposed (Fukatsu, et al., 2004, 2005, 2006). The proposed joints that control the moment consist of the reduced concrete sectional area, short steel ring and joint reinforcement. The reduced concrete sectional area reduces the pile head moment and the steel ring confines the concrete and controls the local destruction of semi-rigid pile head joints. The joint reinforcing bars are used for transmitting of the tension force to a certain amount. The aim of this experimental study is to clarify the structural behaviors in both strength and rotational ductility of the proposed semi-rigid pile head joints.

2. OUTLINE OF EXPERIMENT

2.1. Specimen

The dimensions and reinforcement of the specimen are shown in Fig.1 and the details are shown in Table 1. The reduced concrete sectional area reduces the pile head moment and the steel ring confines the concrete and controls the local destruction of semi-rigid pile head joints. The steel rings are embedded in both piles and stubs. The joint reinforcing bars are used for transmitting the tension force to a certain amount. The joint reinforcing bars of SP1 are welded on the face of the steel rings and those of the other specimens are placed in the steel rings. To consider the construction practice low strength concrete are used in the joint part of SP1~SP5. The embedded length of the steel rings are $D/4$ (D: pile diameter) and $D/20$ for SP1~SP5 and SP6~9, respectively. To decrease the compressive stress the steel rings of SP8 are insulated from the concrete.

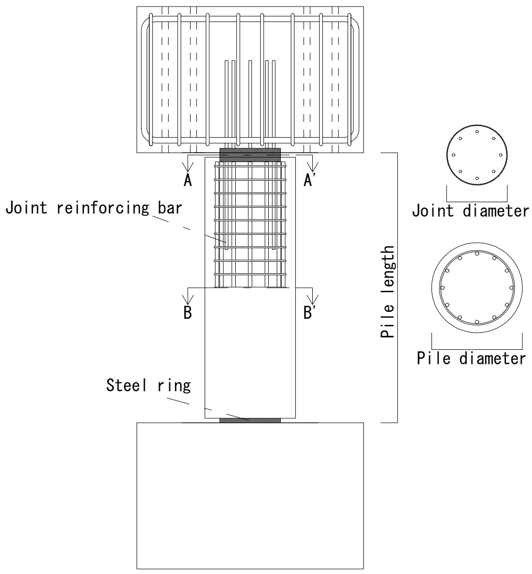

Figure 1 Specimen and reinforcements

Table 1 Specimen details

<table>
<tr><th rowspan="2">Specimen</th><th colspan="2">Joint</th><th colspan="2">Pile</th></tr>
<tr><th>Detail of steel ring</th><th>Joint reinforcing bar</th><th>Body</th><th>Lateral reinforcement</th></tr>
<tr><td>SP1</td><td rowspan="5">Diameter:267.4mm
Thickness:6.0mm
Length:250mm</td><td>Longitudinal:8-D13
Welded on outside of ring
Anchorage:390mm</td><td rowspan="6">Diameter: ϕ 400
Length:1200mm
Longitudinal reinforcement:12-D16</td><td rowspan="6">D6@60
(D6@45: pile top 200mm)</td></tr>
<tr><td>SP2</td><td rowspan="4">Longitudinal:8-D13
Inside of ring
Length:1030mm</td></tr>
<tr><td>SP3</td></tr>
<tr><td>SP4</td></tr>
<tr><td>SP5</td></tr>
<tr><td>SP6</td><td>Diameter:267.4mm
Thickness:3.2mm
Length:60mm</td><td>Longitudinal:8-D13
Position: ϕ 208
Length:840mm</td></tr>
<tr><td>SP7</td><td rowspan="3">Diameter:450mm
Thickness:4.5mm
Length:90mm</td><td rowspan="3">Longitudinal:8-D16
Position: ϕ 364
Length:1050mm</td><td rowspan="3">Diameter: ϕ 600
Length:1440mm
Longitudinal reinforcement:12-D19</td><td rowspan="3">D10@90
(D10@70: pile top 300mm)</td></tr>
<tr><td>SP8</td></tr>
<tr><td>SP9</td></tr>
</table>

2.2. Experimental procedures

The double bending type loading systems are shown in Fig.2. The lateral load is applied to the specimens under a control of relative displacement angles (R) between two end stubs: single cycle at R=1/1000 and 1/400, two cycles at R=1/200, 1/100, 1/50 and 1/25, single cycle at 1/20. The normal stresses applied to the specimens at both piles and joint are shown in Table 2. The variable normal stresses are applied to SP5 and SP9. The high normal stress is applied to SP3 and the tension normal stress is applied to SP4.

Table 2 Normal stress of the specimens

Specimen	Pile (MPa)	Joint (MPa)
SP1,SP2	7.2	16.0
SP3	14.3	32.1
SP4	-2.4	-5.3
SP5	Variable 0～14.3	Variable 0～32.1
SP6	3.6	8.0
SP7,SP8	4.2	7.5
SP9	Variable 0～7.1	Variable 0～12.6

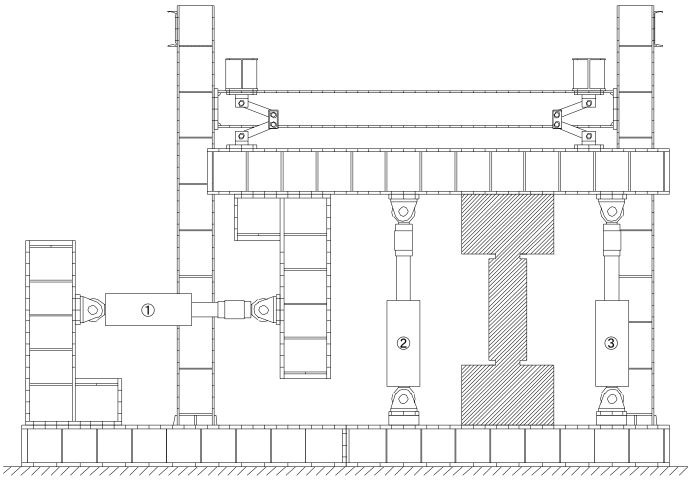

Figure 2 Loading systems

2.3. Materials

The mechanical properties of the concrete and reinforcing bars and rings are shown in Table 3 and Table 4.

Table 3 Mechanical properties of concrete

Use	Compressive strength(MPa)	Tensile strength(MPa)	Young's modulus(GPa)	Specimen
Pile	29.7	-	27.4	SP1,SP2
	31.5	2.95	25.6	SP3,SP4,SP5
	29.8	2.10	30.1	SP6,SP7,SP8,SP9
Joint	20.2	-	-	SP1,SP2
	15.7	1.69	19.1	SP3,SP4,SP5
	29.8	2.10	30.1	SP6,SP7,SP8,SP9

Table 4 Mechanical properties of reinforcing bars and steel rings

Bar type, Ring thickness	Yield strength(MPa)	Tensile strength(MPa)	Young's modulus(GPa)	Use	Specimen
D6	313	492	183	Lateral	SP1,SP2
	432	502	175		ST3,SP3,SP4,SP5
	427	488	180		SP6
D10	369	490	189		SP7,SP8,SP9
D13	354	536	193	Joint	SP1,SP2
	380	542	185		SP3,SP4,SP5
	378	557	182		SP6
D16	427	590	192	Longitudinal	SP1,SP2
	433	578	181		SP3,SP4,SP5
	439	582	181		SP6
	403	564	184	Joint	SP7,SP8,SP9
D19	439	590	184	Longitudinal	SP7,SP8,SP9
t3.2	282	347	192	Steel ring	SP6
t4.5	327	398	201		SP7,SP8,SP9
t6.0	353	451	206*		SP2,SP3,SP4,SP5

*Nominal

3. RESULTS OF EXPERIMENT AND CONSIDERATIONS

3.1. Progress of destructiveness and deformation characteristics

The crack patterns of the specimens at R=1/100 and the final stage of the experiment are shown in Fig. 2. The relationships between the shear load and the displacement of the specimens are shown in Fig. 3. The horizontal crack occurred along the embedded steel ring ends at R=1/200 in SP1. The steel rings pulled out from the concrete stubs due to the bond failure of the steel rings. Because of the yielding of reinforcing steels the failure mode of SP1 was supposed to be the flexural failure of the pile head. SP2 showed about the same behavior as that of SP1. SP3 lost the normal stress support ability at *R*=1/25. The steel rings of SP4 pulled out from the concrete stubs in the early stage at *R*=1/400 with the horizontal cracks. In SP5 the crack pattern similar to SP3 occurred and the maximum shear strength at the minus cycles decreased around 60% of that of the plus cycles.

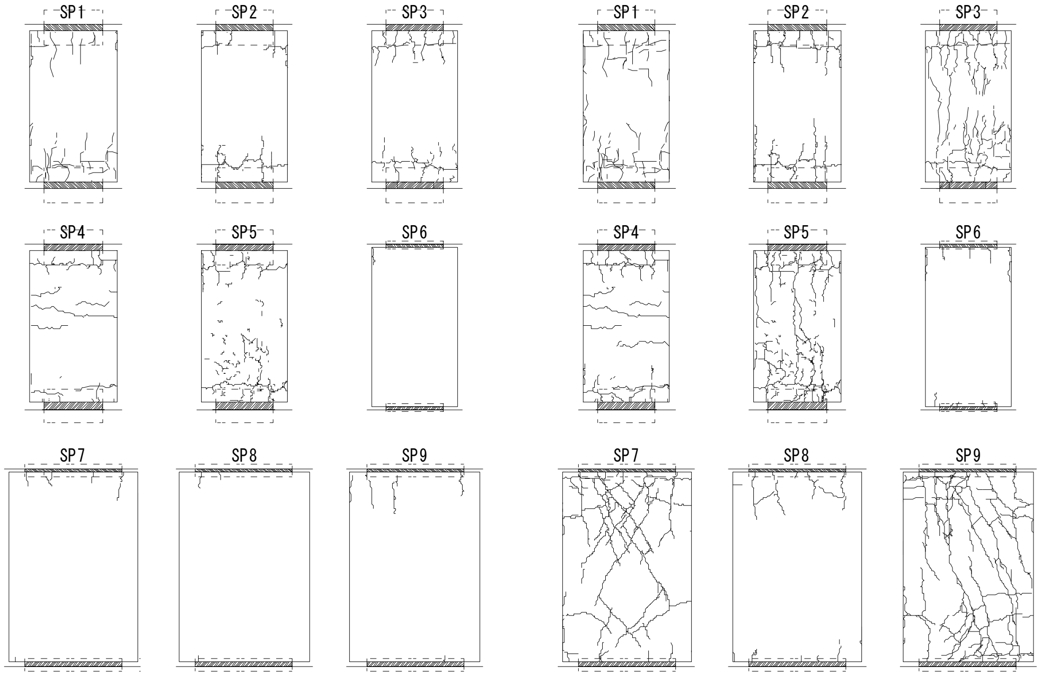

R=1/100 Final

Figure 2 Crack patterns of the specimens

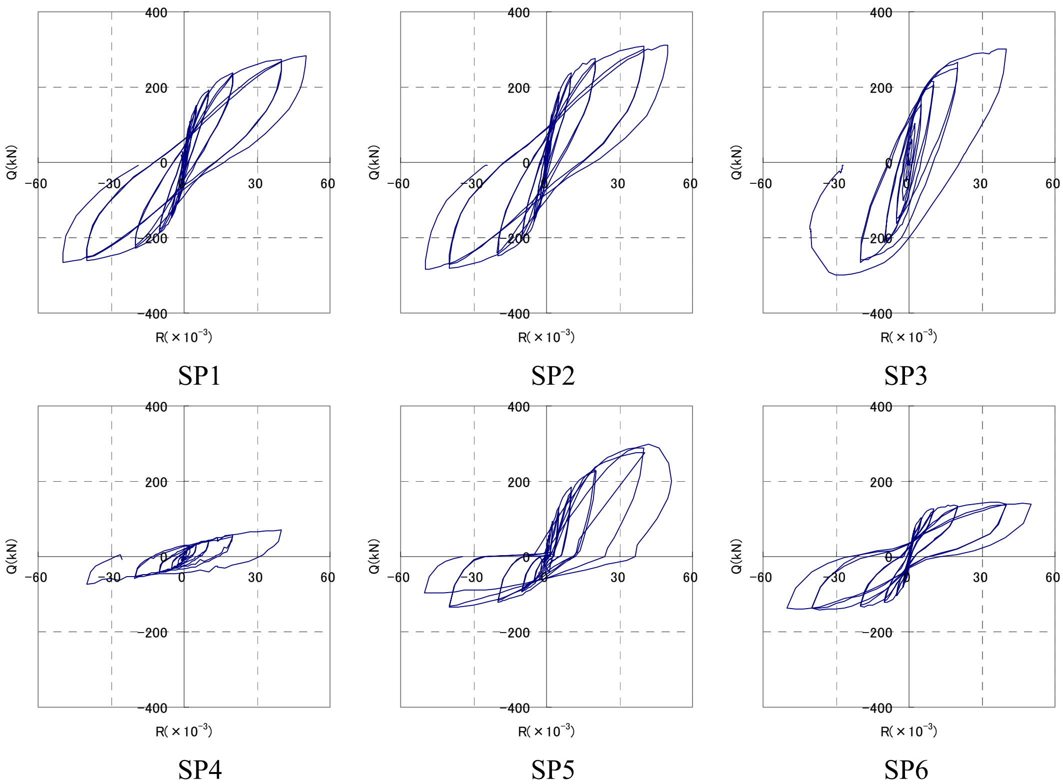

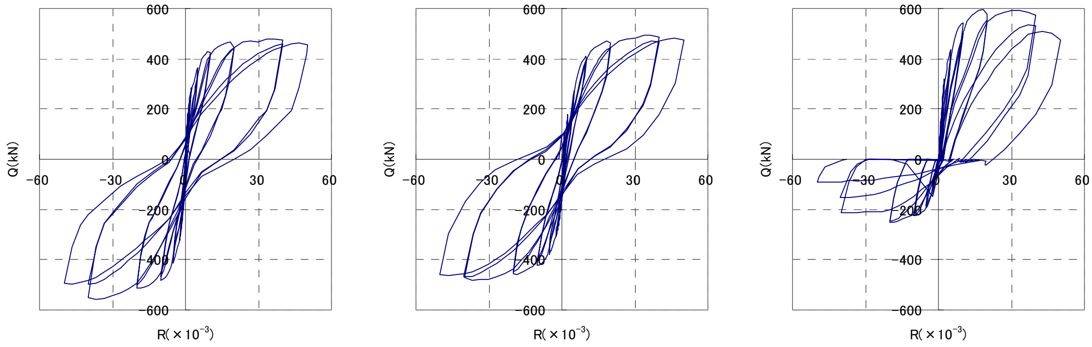

SP7 SP8 SP9

Figure 3 Relationships between shear load and displacement of the specimens

In SP6 the vertical cracks occurred at R=1/100 around the joint part and no cracks in the pile body. In SP7 the shear cracks occurred at R=1/50 due to the tight steel rings. However, in SP8 no shear cracks occurred at higher shear loads due to the effect of the normal stress of insulated steel rings. In SP9 shear cracks occurred at the center of the pile in the plus cycles and flexural cracks occurred in the minus cycles.

3.2. Rotational rigidity

The definitions of rotational rigidity are shown in Fig. 4. The pile head rotational angle is the angle of rotation of the position at 100mm from the pile head. The ratio of rotational rigidity shows the rotational rate of the head joint. In other words the ratio of rotational rigidity becomes 1.0 in the case of the complete rigid body.

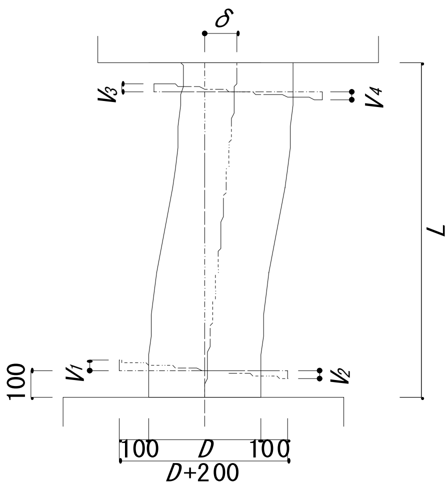

Total rotational angle : $R = \delta / L$
Total rotational rigidity : $K_{\theta 1} = M / R$
Pile head rotational angle : $R_j = \{(V_1+V_2)+(V_3+V_4)\} / 2(D+200)$
Pile head rotational rigidity : $K_{\theta 2} = M / R_j$
Ratio of rotational rigidity : $K = K_{\theta 1} / K_{\theta 2}$

Figure 4 Definitions of rotational rigidity

Table 5 Ratios of rotational rigidity

	+	-
SP1	0.95	0.87
SP2	0.90	0.87
SP3	0.95	0.74
SP4	0.99	0.90
SP5	0.84	0.97
SP6	0.96	0.97
SP7	0.94	0.99
SP8	0.77	1.06
SP9	0.90	0.98

The calculated ratios of rotational rigidity of the specimens are shown in Table 5. The average ratios in the plus and minus cycles at the target angles after R=1/200 are shown, respectively. In the case of semi-rigid pile the ratio of rotational rigidity takes around 0.9. It is confirmed that the rotation concentrates in the pile head joint.

3.3. Ultimate flexural strength

The ultimate flexural strength Q_{mu} are calculated as plane sections remain plane. The stress-strain relationships are expressed in the equation (3.1) considering the confining effect of the steel rings (AIJ, 1977) with the assumption of tensile stress does not occur in the steel rings.

$$\frac{\sigma_c}{{}_c\sigma_{cB}} = \frac{AX + (d-1)X^2}{1 + (A-2)X + dX^2} \tag{3.1}$$

$${}_c\sigma_{cB} = {}_c\sigma_B + k2\alpha t_s \sigma_y / (D - 2t)$$

$$X = \varepsilon_c / \varepsilon_{c0}$$

$$A = E_c \varepsilon_{c0} / {}_c\sigma_{cB}$$

$$K = {}_c\sigma_{cB} / {}_c\sigma_B$$

$$E_c = (0.69 + 0.33\sqrt{{}_c\sigma_B}) \times 10^4$$

$$\frac{\varepsilon_{c0}}{\varepsilon_u} = 1 + 4.7(K-1), K \le 1.5$$

$$\frac{\varepsilon_{c0}}{\varepsilon_u} = 3.35 + 20(K-1.5), K \le 1.5$$

$$d = 1.5 - 0.017\,{}_c\sigma_B + 2.49\sqrt{(K-1)\,{}_c\sigma_B / 23}$$

σ_c, ε_c : normal stress of concrete and strain
${}_c\sigma_{cB}, \varepsilon_{c0}$: strength of confined concrete and strain
${}_c\sigma_B, \varepsilon_u$: concrete strength and strain
E_C : Young's modulus of concrete
k : confined factor (=4.1)
${}_s\sigma_y$: yield strength of steel ring
αt : thickness of steel ring

Table 6 shows the calculated and measured ultimate flexural strength. The ratios of measured flexural strengths to calculated ones of SP1~SP5 (steel ring length=D/20) and SP6~SP9 (steel ring length=D/20) are 1.2~2.0 and 0.9~1.1, respectively. In case of SP6~SP9 the assumptions are in good agreement with the experiment.

Table 6 Ultimate flexural strength

	Calculated		Measured		Ratio	
	+	-	+	-	+	-
	Q_{mu+}	Q_{mu-}	Q_{max+}	Q_{max-}	Q_{max+} / Q_{mu+}	Q_{max-} / Q_{mu-}
ST1	214	-214	259	-210	1.21	0.98
ST2	205	-205	245	-239	1.20	1.17
ST3	270	-86	310	-107	1.15	1.26
SP1	217	-217	283	-267	1.30	1.23
SP2	217	-217	311	-284	1.43	1.31
SP3	244	244	301	-299	1.23	1.22
SP4	37	-37	71	-72	1.95	1.98
SP5	244	-94	299	-135	1.23	1.44
SP6	134	-134	145	-141	1.09	1.06
SP7	500	-500	478	-514	0.96	1.03
SP8	500	-500	493	-481	0.99	0.96
SP9	610	-276	596	-250	0.98	0.91

3.4. Estimation of rotational rigidity

The outer steel strain distributions of SP7 at both plus and minus *R*=1/400, 1/200 and 1/100 are shown in Fig. 5. The strains show the maximum at the center and decrease at a constant rate toward the end. The ultimate flexural strength of SP6~SP7 can be calculated precisely. Based on the strain distributions of the joint reinforcing bars of SP6~SP9 the following equation to estimate the rotational angle is proposed. The relationships between the rotational angles and moment can be calculated from the equation (3.2).

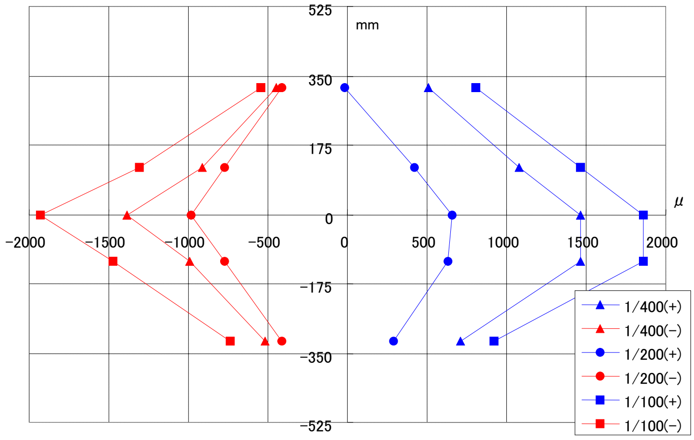

Figure 5 Strain distribution of SP7

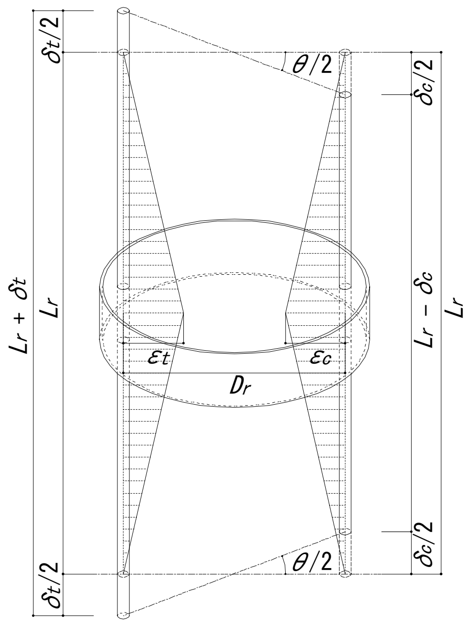

$$\theta = \tan^{-1}(\delta_t - \delta_c) / D_r \tag{3.2}$$

$\delta_t = \varepsilon_t \cdot L_r / 2$

$\delta_c = \varepsilon_c \cdot L_r / 2$

θ : Rotational angle

δ_t : Deformation of reinforcing bar (tension)

δ_c : Deformation of reinforcing bar (compression)

ε_t : Strain of reinforcing bar at the center (tension)

ε_c : Strain of reinforcing bar at the center (compression)

L_r : Length of reinforcing bar

Figure 6 Definitions of rotational angle

The calculated relationships between the rotational angles and moment of SP6~SP9 are shown in Fig. 7. The calculated results are in good agreement with the experimental data. In SP6 the experimental data slightly over the calculated values.

4. CONCLUSIONS

Based on the experimental result and considerations the following conclusions are derived.

1. The proposed semi-rigid pile head joins were able to reduce the moment which occurs to the pile head and

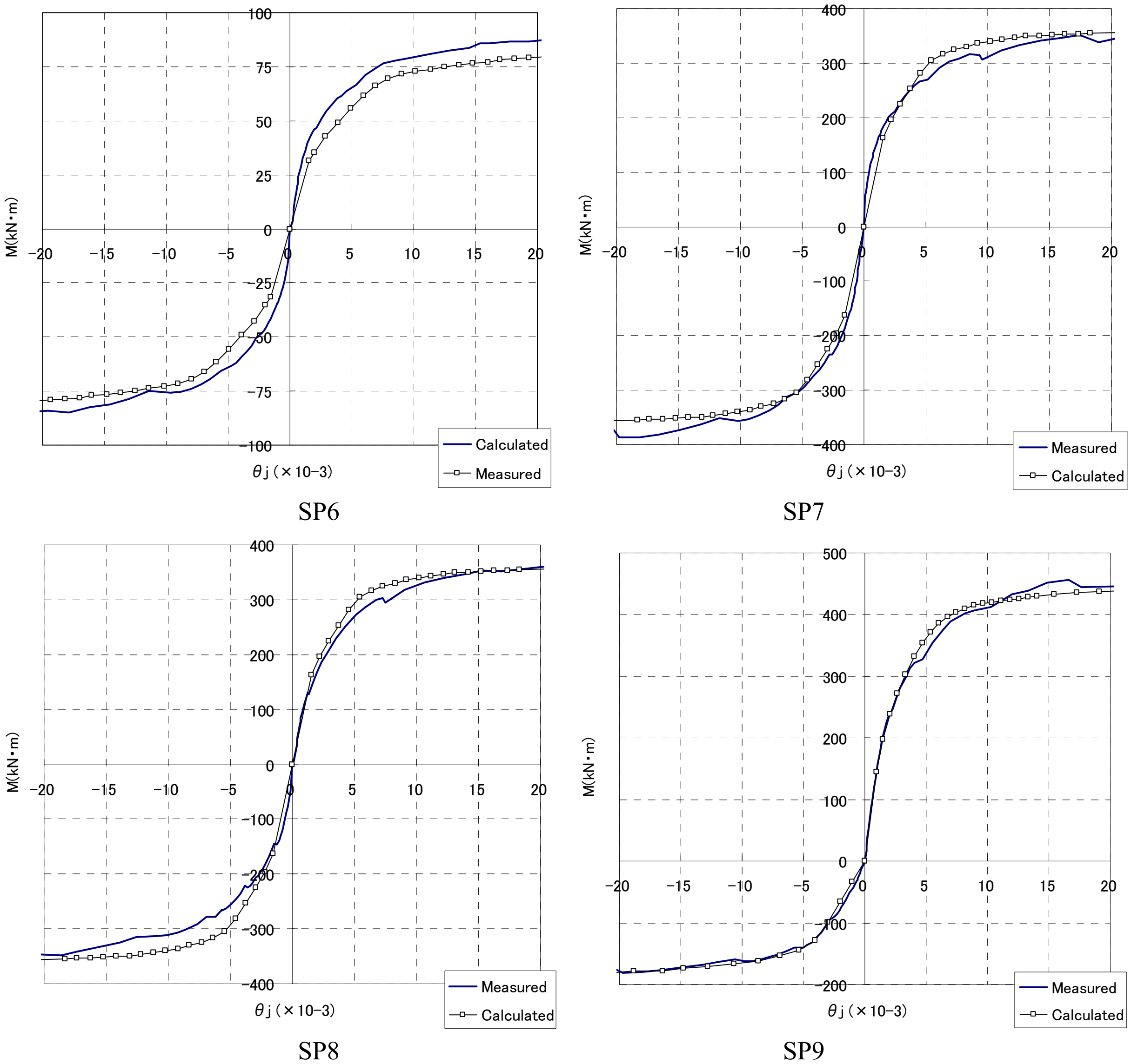

Figure 7 Relationship between rotational angles and moment

the joints satisfied the seismic performance until large deformation.

2. Based on the strain distributions of the joint reinforcing bars a simple way to estimate the rotational rigidity is proposed. The estimated values are in good agreement with the experimental results.

REFERENCES

Yamakata, K. (1996). Damage of building pile foundations in South Hyogo prefecture earthquake and its future measures. *J. of Soil and Foundations* **24:11**, 9-16.

Fukatsu, N., Yamamoto, T., Yamada, K., Okada, T. (2004). An Experimental Study of Semi-rigid Pile Head Joints of Cast-in-Place Concrete Piles. *Proceedings of JCI* **26:2**, 919-924.

Fukatsu, N., Yamamoto, T., Yamada, K., Okada, T. (2005). An Experimental Study of Axial Stress Effect on Semi-rigid Pile Head Joints of Cast-in-Place Concrete Piles. *Proceedings of JCI* ***27:2***, 1633-1638.

Fukatsu, N., Yamamoto, T., Yamada, K., Okada, T. (2006) An Experimental Study of Rotational Rigidity of Semi-rigid Pile Head Joints of Cast-in-Place Concrete Piles. *Proceedings of JCI* ***28:2***, 1669-1674.

AIJ (1977). Standard for Structural Design of Concrete Filled Steel Tube Structures, Japan